

Supplementary Material

1. Turbulent Kinetic Energy Scheme in CCLM

The important part of the 3-D TKE scheme regarding the exchange between atmosphere and ocean is the surface layer. In CCLM this layer is defined as the layer between the ocean surface and the lowest atmospheric model level. This layer is divided into three sub-layers. Starting from the ocean surface upwards these are the laminar layer, the roughness layer and the Prandtl layer. The lower height of the roughness layer begins where the turbulence length is zero and ends at the dynamical roughness length z_0 . As a closure condition, the one developed by [1, 2] is applied. The roughness length of momentum over water surfaces is calculated by the Charnock formula [3]:

$$z_{0m} = \frac{\alpha_c}{g} (u_*^2 + w_*^2) \quad (1)$$

A value of 0.015 is used for α_c over open water in Equation (1). u_* is the friction velocity, and w_* is the scaling velocity for free convection. In case of unstable conditions, $w_*=0$. The roughness length is limited to values lower than half of the lower layer thickness. Over sea ice, the roughness length is set to a constant value $z_{0m}=0.001\text{m}$.

The roughness length for heat is defined as

$$z_{0h} = \min\left(\frac{g * \nu * \alpha_h}{\max(10^{-8}, u_*)}, 0.98\right) \quad (2)$$

where $\nu=1.5\text{E-}5$ is the kinematic viscosity constant and a value of 0.6 is used for α_h . In Equation (2), $z_{0h} = z_{0m}$ over sea ice.

These roughness lengths are then used to calculate the turbulent diffusion coefficients for momentum and heat. Since u_* and w_* depend on the roughness length itself, an additional iterative step is performed to calculate the final roughness length and turbulent diffusion coefficients for momentum and heat. The latter are used to compute the fluxes for momentum and heat/moisture at the surface between atmosphere and ocean [4].

2. Parameterizations in NEMO

A detailed description of the CORE bulk formulae estimating the air-sea fluxes within the NEMO model is given in [5]. The following text highlights some specialities of the CORE equations, which are of interest for the presented study.

Large and Yeager [5] showed that bulk formulae effectively transform the problem of specifying the turbulent surface fluxes in the near-surface atmospheric state (wind, U , temperature, θ , and humidity, q) by utilizing fitted transfer coefficients. One challenge in forcing oceanic global models (OGCMs) is that the estimates for the atmospheric values are often not given at the same heights, which makes the usage of fixed transfer coefficients inappropriate. In the NEMO CORE formulae the drag coefficient, C_D , and the transfer coefficients for evaporation, C_E , and sensible heat, C_H , are functions of height, z , atmospheric stability ζ , and wind speed. The equations for the surface stress, $\vec{\tau}$, evaporation, E , and sensible heat, Q_H , are then defined as:

$$\vec{\tau} = \rho_a C_D(z, \zeta, U) |\Delta\vec{U}| \Delta\vec{U} \quad (3)$$

$$E = \rho_a C_E(z, \zeta, U) \left(q(z_q) - q_{\text{sat}}(\text{SST}) \right) |\Delta\vec{U}| \quad (4)$$

$$Q_H = \rho_a c_p C_H(z, \zeta, U) (\theta(z_\theta) - \text{SST}) |\Delta\vec{U}| \quad (5)$$

where ρ_a is the air density, c_p is the specific heat of the air, and $\Delta\vec{U}$ is the vector difference between the surface current and the wind at height of the wind estimate, z_U . z_q and z_θ are the height of the humidity and temperature estimates. The advantage of the adaptive transfer coefficients is that it is more flexible in accepting forcing from different sources, e.g. in coupled model setups, and the efficiency of the calculation increases [5]. In Equations (3)–(5), under neutral stability, the 10 m values of the transfer coefficients are given by following Equations (6)–(9)

$$1000C_D = \frac{2.70 \text{ [m/s]}}{U_N(10\text{m})} + 0.142 + \frac{U_N(10\text{m})}{13.9 \text{ [m/s]}} \quad (6)$$

$$1000C_E = 34.6\sqrt{C_D} \quad (7)$$

$$1000C_H = 18.0\sqrt{C_D}, \quad \text{stable } \zeta > 0 \quad (8)$$

$$1000C_H = 32.7\sqrt{C_D}, \quad \text{unstable } \zeta \leq 0 \quad (9)$$

The height and stability dependent conversion of the transfer coefficients is archived over an iterative approach using two to five iterations. We refer the interested reader to the original work of [5] and the references therein.

The bottom friction uses a spatially varying log layer with a minimum drag coefficient set to 1×10^{-6} for the Danish Straits and the Baltic Sea and 4×10^{-3} for the rest of the setup domain. The tracer advection uses a TVD approach with the total variance decreasing scheme [6] and a 2D varying Laplacian diffusion operator with a value of $0.25 \text{ m}^2/\text{s}$ for the region covering the Danish Straits and the Baltic Sea, and a value of $50 \text{ m}^2/\text{s}$ for the rest of the setup domain. The Craig and Banner surface wave mixing parameterization [7] is used with a wave breaking TKE flux of 50 and the dissipation under stratification is limited using a Galperin limit of 0.07 [8].

3. Surface energy balance

The calculation of the energy balance at the surface is a common method in climate research. It comprises the balancing equation of energy fluxes at the surface (e.g., Anber et al. [9]):

$$SW + LW - LH - SH - G = 0 \quad (10)$$

In Equation (10), SW and LW are the net absorbed shortwave radiative flux and the net longwave radiative flux (W/m^2) which are defined in Equations (11) and (12), respectively:

$$SW = SW \downarrow - SW \uparrow \quad (11)$$

$$LW = LW \downarrow - LW \uparrow \quad (12)$$

where $SW \downarrow$ and $SW \uparrow$ are downward and upward solar radiative fluxes, $LW \downarrow$ and $LW \uparrow$ are downward and upward long-wave radiative fluxes at the surface. In Equation (10), LH is the surface latent heat flux, SH is the surface sensible heat flux and G is ground heat flux (or heat conducted away from the surface). G is defined by Equation (13) as following:

$$G = \rho H C \frac{dT}{dt} \quad (13)$$

over water T is sea surface temperature, ρ is water density ($1000 \text{ kg}/\text{m}^3$), C is the heat capacity of water ($4180 \text{ J}/\text{kg}/\text{K}$), H is the depth of the mixed layer.

Net radiation Rnet is balanced by sensible, latent and conduction heat fluxes:

$$R_{\text{net}} = SW \downarrow + LW \downarrow - SW \uparrow - LW \uparrow = LH + SH + G \quad (14)$$

meaning the energy amount gained by radiation is equal to the heat loss via latent, sensible and ground heat fluxes. Therefore, if Rnet is positive downward, LH, SH and G are positive upward. However, in CCLM and many other models, these kinds of energy fluxes are defined with the same sign. To make it easier to interpret the results, we define LWFX = -LH and SHFL = -SH.

The ground heat flux G from Equation (14), therefore, can be calculated as:

$$G = R_{\text{net}} - LH - SH = R_{\text{net}} + \text{LHFX} + \text{SHFL} \quad (15)$$

The right hand side of the Equation (15) is considered as the net surface energy flux Qnet (also see Dieterich et al. [10]). A change in Qnet will alter G and, therefore, lead to a change in surface temperature T.

Table S1. Variables exchanged between compartment models in GCOAST-AHOI. S: information is sent; R: information is received.

Variable (unit)	CCLM	NEMO+LIM3	HD
Mean sea level pressure (Pa)	S	R	
10-M U-wind component (m/s)	S	R	
10-M V-wind component (m/s)	S	R	
Surface U-momentum flux (N/m ²)	S	R	
Surface V-momentum flux (N/m ²)	S	R	
Surface solar downward radiation flux (W/m ²)	S	R	
Surface longwave downward radiation flux (W/m ²)	S	R	
2-M air temperature (K)	S	R	
2-M air specific humidity (kg/kg)	S	R	
Precipitation (kg/m ² /s)	S	R	
Snow (kg/m ² /s)	S	R	
Latent heat flux (W/m ²)	S	R	
Sensible heat flux (W/m ²)	S	R	
Surface runoff (kg/m ² /hr)	S		R
Sub-surface runoff (kg/m ² /hr)	S		R
Sea surface temperature (K)	R	S	
Sea ice fraction (0–1)	R	S	
Sea ice albedo (0–1)	R	S	
Discharge (m ³ /s) River runoff (kg/m ² /s)		R	S

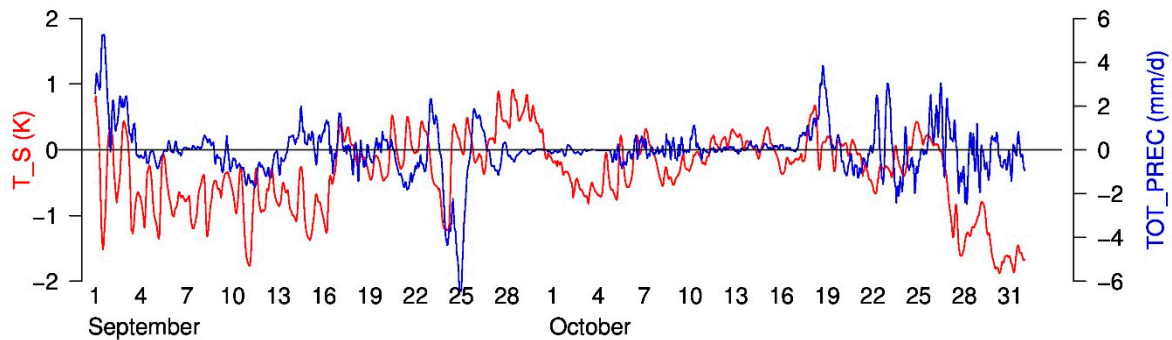


Figure S1. Difference of hourly surface temperature T_S (K, red line) and precipitation TOT_PREC (mm/d, blue line) averaged over land points of the NoEU area between CCLM1 and CCLM4. Time period: 01 September–31 October 2013.

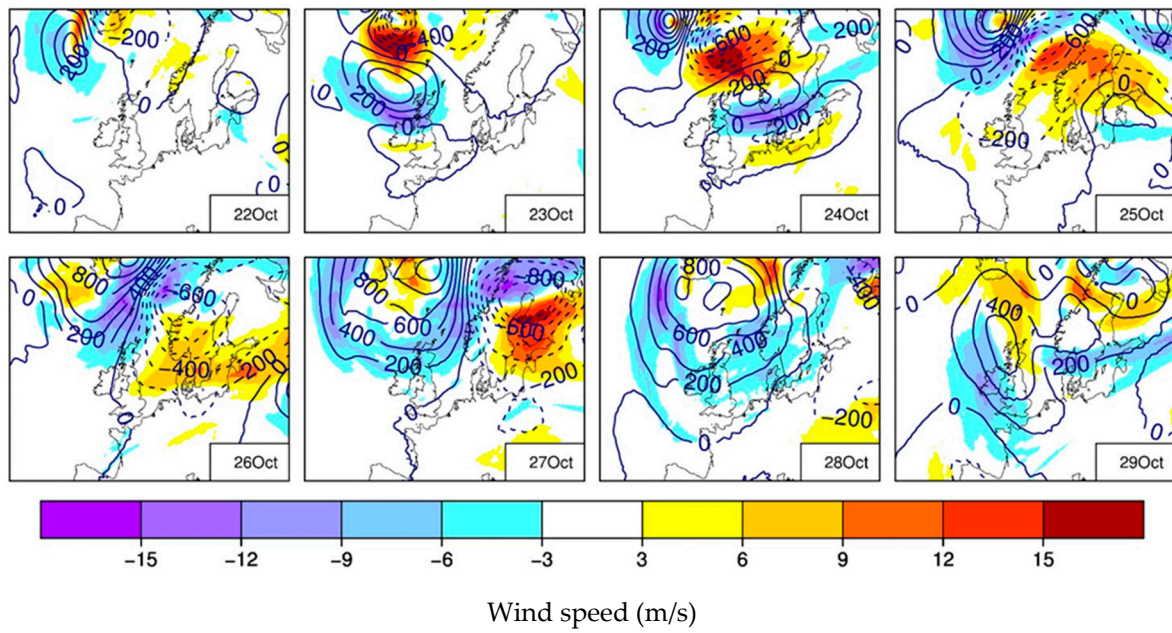


Figure S2. Difference of daily mean geopotential height (gpm, contour) and wind speed (m/s, shaded) at 500mb between CCLM1 and CCLM4. Time period: 22–29 October 2013.

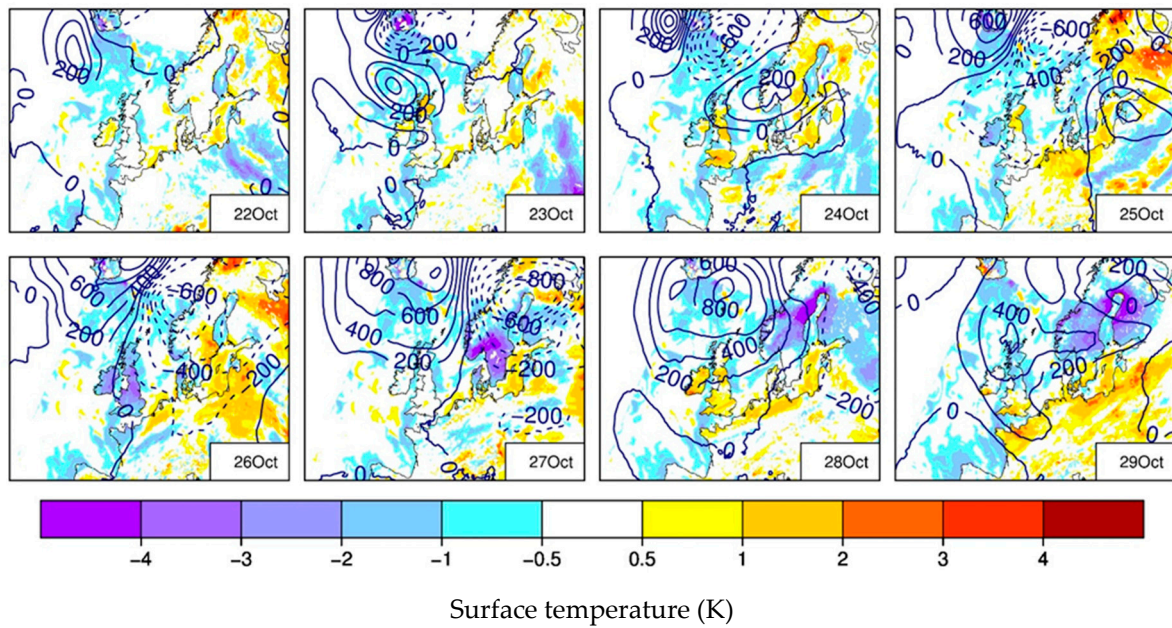


Figure S3. Difference of daily mean geopotential height at 500mb (gpm, contour) and T_S (K, shaded) between CCLM1 and CPL0. Time period: 22–29 October 2013.

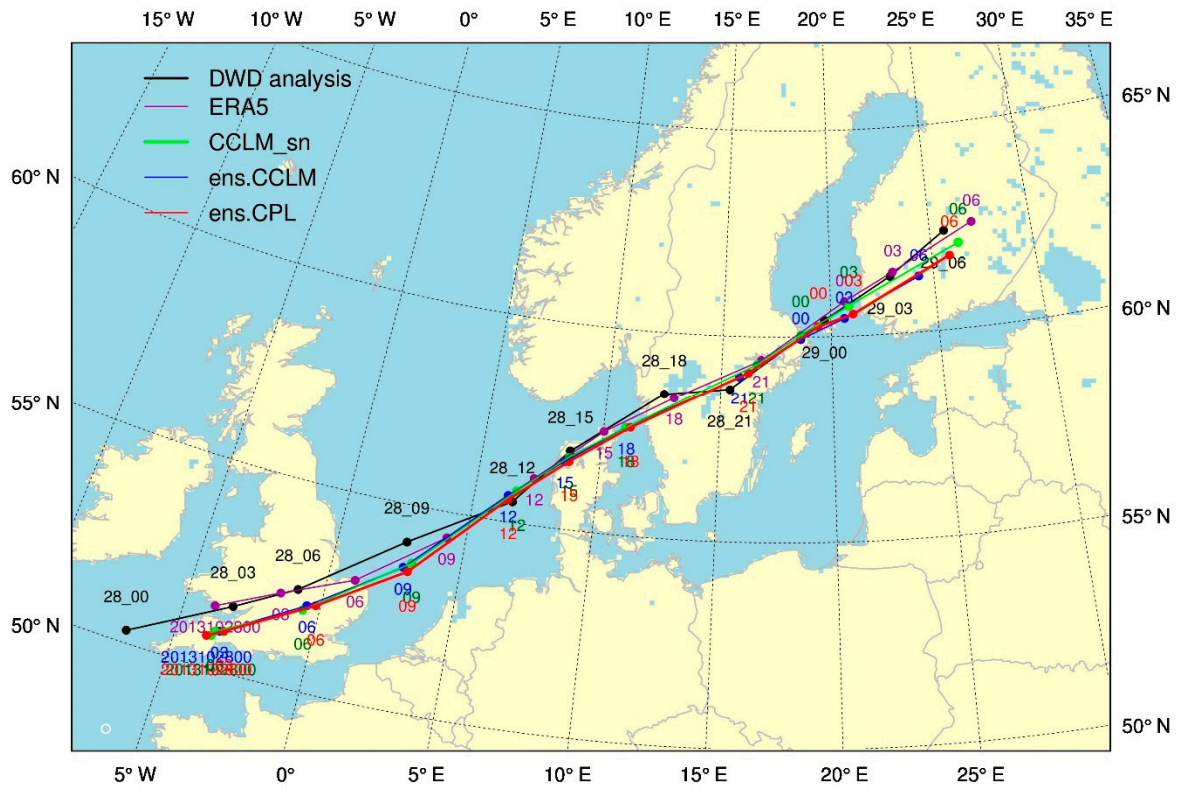


Figure S4. Storm tracks from DWD (Deutscher Wetterdienst, German National Meteorological Service), ERA5 reanalysis data, CCLM_sn, ens.CCLM and ens.CPL. Time: 3-hourly from 00 UTC 28 October 2013 to 06 UTC 29 October 2013.

References

1. Mellor, G.L.; Yamada, T. A Hierarchy of Turbulence Closure Models for Planetary Boundary Layers. *J. Atmos. Sci.* **1974**, *31*, 1791–1806. doi:10.1175/1520-0469(1974)031<1791:ahotcm>2.0.co;2.
2. Mellor, G.L.; Yamada, T. Development of a turbulence closure model for geophysical fluid problems. *Rev. Geophys.* **1982**, *20*, 851–875. doi:10.1029/RG020i004p00851.
3. Charnock, H. Wind stress on a water surface. *Quart. J. Roy. Meteor. Soc.* **1955**, *81*, 639–640. doi:10.1002/qj.49708135027.
4. Doms, G.; J., F.; Heise, E.; Herzog, H.J.; Mrionow, D.; Raschendorfer, M.; Reinhart, T.; Ritter, B.; Schrodin, R.; Schulz, J.P.; Vogel, G. A description of the nonhydrostatic regional COSMO model. Part II: Physical parameterization. Technical report, Deutscher Wetterdienst, 2011. Available at <http://www.cosmo-model.org/content/model/documentation/core/cosmoPhysParamtr.pdf>, Accessed: 2014-04-09.
5. Large, W.G.; Yeager, S. Diurnal to decadal global forcing for ocean and sea-ice models: the data sets and flux climatologies. Technical Note NCAR/TN-460+STR, CGD Division of the National Center for Atmospheric Research, NCAR, 2004.
6. Zalesak, S.T. Fully multidimensional flux-corrected transport algorithms for fluids. *J. Comput. Phys.* **1979**, *31*, 335–362. doi:10.1016/0021-9991(79)90051-2.
7. Craig, P.D.; Banner, M.L. Modeling wave-enhanced turbulence in the ocean surface layer. *J. Phys. Oceanogr.* **1994**, *24*, 2546–2559. doi:10.1175/1520-0485(1994)024<2546:mwetit>2.0.co;2.
8. Galperin, B.; Kantha, L.H.; Hassid, S.; Rosati, A. A quasi-equilibrium turbulent energy model for geophysical flows. *J. Atmos. Sci.* **1988**, *45*, 55–62. doi:10.1175/1520-0469(1988)045<0055:aqetem>2.0.co;2.
9. Anber, U., S. Wang, and A. Sobel. Coupling with ocean mixed layer leads to intraseasonal variability in tropical deep convection: Evidence from cloud-resolving simulations, *J. Adv. Model. Earth Syst.* **2017**, *9*, 616–626, doi:10.1002/2016MS000803.
10. Dieterich, C.; Wang, S.; Schimanke, S.; Gröger, M.; Klein, B.; Hordoir, R.; Samuelsson, P.; Liu, Y.; Axell, L.; Höglund, A.; Meier, H.E.M. Surface heat budget over the North Sea in climate change simulations. *Atmosphere* **2019**, *10*, 272. doi:10.3390/atmos10050272.

Part 1: “Turbulent Kinetic Energy Scheme in CCLM”, Part 2: “Parameterizations in NEMO”, Part 3: “Surface energy balance”, Table S1: “Variables exchanged between compartment models in GCOAST-AHOI. S: information is sent; R: information is received”, Figure S1: “Difference of hourly surface temperature T_S (K, red line) and precipitation TOT_PREC (mm/d, blue line) averaged over land points of the NoEU area between CCLM1 and CCLM4. Time period: 01 September–31 October 2013.”, Figure S2: “Difference of daily mean geopotential height (gpm, contour) and wind speed (m/s, shaded) at 500mb between CCLM1 and CCLM4. Time period: 22–29 October 2013.”, Figure S3: “Difference of daily mean geopotential height at 500mb (gpm, contour) and T_S (K, shaded) between CCLM1 and CPL0. Time period: 22–29 October 2013.”, Figure S4: “Storm tracks from DWD (Deutscher Wetterdienst, German National Meteorological Service), ERA5 reanalysis data, CCLM_sn, ens.CCLM and ens.CPL. Time: 3-hourly from 00 UTC 28 October 2013 to 06 UTC 29 October 2013.”.